J|A|C|S
ARTICLES
Published on Web 05/04/2002

Structure and Thermodynamics of Carbon and Carbon/Silicon Precursors to Nanostructures

Vassiliki-Alexandra Glezakou,[†,‡] Jerry A. Boatz,[§] and Mark S. Gordon*[,||]

Contribution from the San Diego Supercomputer Centre, University of California San Diego, 9500 Gilman Drive, MC0505, La Jolla, California 92093-0505, Air Force Research Laboratory AFRL/PRS, Edwards AFB, California 93524-7680, and Department of Chemistry, Iowa State University, Ames, Iowa 50011

Received October 4, 2001

Abstract: The structures at the Hartree−Fock level, as well as the energetics, are reported for the unsaturated system $C_{36}H_{16}$, its Si-doped analogue $C_{32}Si_4H_{16}$, and several smaller, unsaturated fragments. Structural effects on the electronic distribution are discussed in terms of a localized orbital energy decomposition. The standard heats of formation are calculated based on homodesmic and isodesmic reactions and the G2(MP2,SVP) method with a valence double-ζ plus polarization basis. The origin of the observed explosion of the all-carbon system ($C_{36}H_{16}$) to form carbon nanotubes was investigated by exploring a possible initial reactive channel (dimerization), which could lead to the formation of the observed onion-type nanostructures.

Introduction

In this paper, the structure and standard heat of formation of the annulene derivative, $C_{36}H_{16}$ (1,2:5,6:11,12:15,16-tetrabenzo-3,7,9,13,17,19-hexadehydro[20]annulene) and that of its Si-doped isomer $C_{32}Si_4H_{16}$ (1,2:5,6:11,12:15,16-tetrabenzo-3,7,9,13,17,19-hexadehydro-8,9,18,19-tetrasila[20]annulene) are reported. The synthesis and properties of the parent system were reported recently:[1] this system is quite stable and inert to irradiation but readily explodes in a vacuum under mild heating to give pure carbon nanotubes. X-ray diffraction studies and semiempirical MNDO-PM3 calculations suggest a chiral conformation with an isomerization barrier through a planar structure that is only 7.5 kcal mol^{-1} higher than the ground state. As various experiments suggest,[2] this material may present new opportunities in C or non-C nanostructures.

The current work explores the following: (a) The thermodynamics of the parent molecule was investigated. (b) The structural and thermodynamic effects of partial substitution in the C backbone by Si. Si-doped polymers have been proposed in the literature to interpret Si surfaces.[3] In 1981, the first Si═Si-containing compound was synthesized,[4a] the same year that the first Si═C-containing species was also isolated.[4b] Although Si and C are congeners, Si- or Si-doped two-dimensional polymers still evade detection. Nonetheless, as silicon semiconductors become smaller and smaller, theoretical investigation of Si-doped systems, both small and large, can be very helpful.[5] The readiness with which the all-carbon system transforms into onion-type nanotubes[6] (concentric spherical nanocapsules) may present researchers with a possible pathway to obtain Si-doped nanostructures, once the $C_{32}Si_4H_{16}$ parent has been synthesized. (c) A possible reactive channel, dimerization of the parent compound, for the first step in the explosive transformation to nanostructures and a comparison to the "chicken wire" isomer $C_{36}H_{16}$ is explored.

The present theoretical treatment also presents an evaluation of a reduced computational requirement method for thermochemical predictions. Such predictions on large systems or systems with delocalized electrons often give contradicting results.[7]

Computational Details

In the present work, the G2 suite of methods for small reference compounds is combined with homodesmic reactions to estimate heats of formation for the molecules of interest.

The G2 methodology[8] is one of several theoretical chemical models that aim at providing reliable energies (within ~5 kcal mol^{-1}) through

* To whom correspondence should be addressed. E-mail: mark@si.fi.ameslab.gov.
† University of California San Diego.
‡ E-mail: vanda@si.fi.ameslab.gov.
§ Edwards AFB.
|| Iowa State University.

(1) Boese, R.; Matzger, A. J.; Vollhardt, K. P. C. *J. Am. Chem. Soc*. **1997**, *119*, 2052.
(2) (a) Diederich, F. In *Modern Acetylene Chemistry*; Stang, P. J., Diederich, F., Eds.; VCH: Weinheim, 1995. (b) Tobe, Y.; Fujii, T.; Matsumoto, H.; Naemura, K. *Pure Appl. Chem*. **1996**, *68*, 239. (c) Kuwatani, Y.; Ueda, I. *Angew. Chem., Int. Ed. Engl*. **1995**, *34*, 1892. (d) Zhou, Q.; Carroll, P. J.; Swager, T. M. *J. Org. Chem*. **1994**, *59*, 1294.
(3) Padney, *Phys. Rev. Lett.* **1981**, *28*, 1913. (b) Private communication.
(4) (a) West, R.; Fink, M. J.; Michl, J. Science, **1981**, *214*, 1343. (b) Brok, A. G.; Abdesaken, F.; Gutenkunst, B.; Gutenkunst, A.; Kallury, R. K. *Chem. Soc.* **1981**, *191*, 1981.
(5) (a) Bakshi, A. K. *Solid State Commun.* **1993**, *88*, 401 and references therein. (b) Mann, J. *The Structure, Dynamics, and Function of Interfaces, and Thin Films*; 1st Hansen Lecture, Physcial Chemistry Seminar, Iowa State University, Spring 1999.
(6) (a) Dresselhaus, M. S.; Dresselhaus, G.; Eklund, P. C. *Science of Fullerenes and Carbon Nanotubes*; Academic Press: San Diego, CA, 1996. (b) Ebbesen T. W. *Phys. Today* **1996** (June).
(7) Diederich, F.; Rubin, Y. *Angew. Chem., Int. Ed. Engl.* **1992**, *31*, 1101.
(8) Curtiss, L. A.; Raghavachari, K.; Trucks, G. W.; Pople, J. A. *J. Chem. Phys.* **1991**, *94*, 7221.

10.1021/ja012301u CCC: $22.00

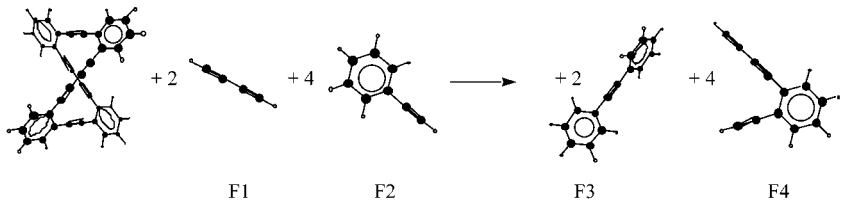

Figure 1. Homodesmic reaction for $C_{36}H_{16}$.

a series of ab initio calculations that include correlation. In this procedure, the quadratic configuration interaction energy with single and double excitations and perturbative triples[9] and an extended basis set, QCISD(T)/6-311+G(3df,2p), is approximated through various levels of second- and fourth-order perturbation theory and a variety of increasingly larger basis sets. However, even in this approximation, the calculations soon become impossible for large systems. Therefore, a number of alternative "G2-like" schemes with reduced basis set and level of theory requirements[10] have been devised that appear to give the same level of accuracy but in a more economical manner.

The G2(MP2,SVP)[10b] theory was chosen for the present work, with a split-valence plus polarization (SVP, 6-31G(d)) basis set employed for the optimizations at the Hartree−Fock level and for the second derivatives of the energy. A second optimization is performed at the MP2-FU//6-31G(d) (full core) level of theory. The final G2(MP2,SVP) energy combines single-point calculations at the MP2 geometries and includes two steps: (I) an MP2 calculation with an extended basis set to obtain the effect of the large basis sets; (II) a quadratic configuration interaction calculation with singles, doubles, and (perturbative) triples (QCISD(T)).

The total G2(MP2, SVP) energy is given by the following formula:

$$E_0 = E[\text{QCISD(T)/6-31G(d)}] + \Delta(\text{MP2,SVP}) + \text{HLC} + E(\text{ZPE}) \quad (1)$$

where

$$\Delta(\text{MP2,SVP}) = E[\text{MP2/6-311+G(3df,2p)}] - E[\text{MP2/6-31G(d)}]$$

is the change in the second-order perturbation theory (MP2) energy due to the basis set improvement.

The higher level correction (HLC) is computed in the same manner as in the original G2 method, and the zero-point energy (ZPE) correction is evaluated from the Hartree−Fock force fields scaled by 0.893.[11] This procedure has been shown to yield considerable savings in both disk space and CPU time without sacrificing the reliability of the original scheme.

All calculations were performed with the Gaussian94,[12] GAMESS,[13] and ACESII[14] quantum chemistry codes.

Homodesmic and Isodesmic Reactions. Homodesmic and isodesmic reactions[15] are schemes that help optimize the cancellation of systematic errors. They are balanced chemical reactions that break a large molecule into smaller fragments, on which high-level calculations are feasible. A *homodesmic* reaction balances the number and the formal type of the chemical bonds involved, maintaining at the same time the connectivity of atoms and groups. An *isodesmic* reaction usually preserves only the number of bond types, and hydrogens are used to terminate the fragments. The typical error of the "conventional" G2 procedure[8] for the computed heats of formation is 2−3 kcal mol^{-1}, which increases with the number of heavy atoms. Raghvachari et al.[14] argued that isodesmic reactions are more reliable for larger systems, as long as G2 energies are used on both sides. In general, the homodesmic scheme is preferable when possible, especially when G2 energies are not available, because the cancellation of errors is more uniform. Experimental heats of formation may also be used for reference molecules in these schemes, to obtain more accurate heats of formation, for target molecules.

For the system $C_{36}H_{16}$, the gas-phase standard heat of formation is evaluated using the homodesmic reaction as shown in Figure 1. For the Si-doped systems, simpler isodesmic reactions are used, because these isomers have a more complicated morphology, as will be shown below. Further details regarding the computation are given in the following sections.

Results

A. Structure, G2(MP2,SVP) Energy, and Heat of Formation of the Primary Fragments. The G2(MP2,SVP) energies for a number of small hydrocarbons and silanes were calculated for use in the appropriate reactions, for the theoretical prediction of their gas-phase standard heats of formation at 298.15 K. Figure 1 outlines the homodesmic reaction used for the evaluation of the $C_{36}H_{16}$ system, at the G2(MP2, SVP) level of theory. The thermochemical data obtained in this section are used in sections B−D for the prediction of the heats of formation of the larger systems. The total MP2 (full core) optimized energies at 6-31G(d), and the single-point MP2/6-31G(d)// $MP2^{FC}$/6-31G(d), MP2/6-311+(3df,2p)// $MP2^{FC}$/6-31G(d), and QCISD(T)/6-31G(d)// $MP2^{FC}$/6-31G(d) energies of the primary fragments are available as Supporting Information, Table S1. Table 1 presents the MP2 geometries for the C/H fragments. The Si-doped fragments seem to be more sensitive to the level of theory as can be evinced from Tables 2 and 3 (see Figure 2 for connectivity of atoms in these systems).

The Si-containing molecules have open-shell ground states. The G2 procedure treats open-shell systems within the unrestricted formulation. We have treated these systems with both

(9) K. Raghavachari, G. W. Trucks, J. A. Pople, M. Head-Gordon *Chem. Phys.* **1989**, *157*, 479.
(10) (a) For G2(MP2): Curtiss, L. A.; Raghavachari, K.; Pople, J. A. *J. Chem. Phys.* **1993**, *98*, 1293. (b) For G2(MP2, SVP): Smith, B. J.; Radom, L. *J. Phys. Chem.* **1995**, *99*, 6468. (c) For G2(MP2, SV): Curtiss, L. A.; Redfern, P. C.; Smith, B.; Radom, L. *J. Chem. Phys.* **1996**, *104*, 5148. (d) For the conventional G3 method, see: Curtiss, L. A.; Raghavachari, K.; Redfern, P. C.; Rassolov, V.; Pople, J. A. *J. Chem. Phys.* **1998**, *109*, 7764 and references 1−4 therein for the older G1 and G2 methods.
(11) Pople, J. A.; Scott, A. P.; Wong, M. W.; Radom, L. *Isr. J. Chem.* **1993**, *33*, 345.
(12) Gaussian 94, Revision D.1: Frisch, M. J.; Trucks, G. W.; Schlegel, H. B.; Gill, P. M. W.; Johnson, B. J.; Robb, M. A.; Cheeseman, J. R.; Keith, T. A.; Petersson, G. A.; Montgomery, J. A.; Raghavachari, K.; Al-Laham, M. A.; Zakrzewski, V. G.; Ortiz, J. V.; Foresman, J. B.; Cioslowski, J.; Stefanov, B. B.; Nanayakkara, A.; Challacombe, M.; Peng, C. Y.; Ayala, P. Y.; Chen, W.; Wong, W.; Andres, J. L.; Replogle, E. S.; Gomberts, R.; Martin, R. L.; Fox, D. J.; Binkley, J. S.; DeFrees, D. J.; Baker, J.; Stewart, J. P. P.; Head-Gordon, M.; Gonzalez, C.; Pople, J. A. Gaussian Inc., Pittsburgh, PA, 1995.
(13) GAMESS: Schmidt, M. W.; Baldridge, K. K.; Boatz, J. A.; Elbert, S. T.; Gordon, M. S.; Jensen, J. H.; Koseki, S.; Matsunaga, N.; Nguyen, K. A.; Su, S. J.; Windus, T. L.; Dupuis, M.; Montogomery, J. A. *J. Comput. Chem.* **1993**, *14*, 1347.
(14) ACESII, product of the Quantum Theory Project, University of Florida, by: Stanton, J. F.; Gauss, J.; Watts, J. D.; Nooijen, M.; Oliphant, N.; Perrera, S. A.; Szalay, W. J.; Lauderdale, W. J.; Gwaltney, S. R.; Beck, S.; Balkova, A.; Bernhold, D. E.; Baeck, K.-K.; Rozyczko, P.; Sekino, H.; Huber, C.; Bartlett, R. J. Integral Packages: VMOL (Almlöf, J.; Taylor, P. R.); VPROPS (Taylor, P. R.); ABACUS (Helgaker, T.; Jensen, H. J. Aa.; Jorgensen, P.; Olsen, J.; Taylor, P. R.).
(15) (a) George, P.; Trachtman, M.; Bock, C. W.; Brett, A. M. *Tetrahedron* **1976**, *32*, 317. (b) Hehre, W. J.; Rarom, L.; Schleyer, P. v. R.; Pople, J. A. *Ab Initio Molecular Orbital Theory*; Wiley: New York, 1986.

Table 1. MP2/6-31G(d) Selected Geometrical Parameters for C/H Species (Distances in Å, Angles in deg)

molecule	CC (triple)	C–C	C–H	∠HCH	∠HCC	dihedral
CH_4			1.084	109.5		
C_2H_2		1.245	1.056			
C_2H_4		1.317	1.076	121.8	116.4	
C_3H_6 (D_3d)		1.527	1.086	107.7	111.2	
C_4H_2	1.187	1.389	1.057			
C_6H_6		1.386	1.076		120.0	
$C_6H_5-C_2H$	1.188	1.386				
		1.443 ($C_{Ph}-C_2$)				
o-$HC_2-C_6H_4-C_4H$	1.190 (av)	1.390	1.076			
		1.438 ($C_{Ph}-C_4H$)				
		1.387 (CC−CC)				
		1.440(C_{Ph}-C_2H)				
C_6H_5-CC−C_6H_5	1.192	1.390				−100.1
		1.443(C_{Ph}-CC)				

Table 2. Selected $C_2H_2Si_2$ Geometrical Parameters at Various Levels of Theory[a]

	SCF				MP2		
	RHF/ROHF			UHF	RMP2		UMP2
parameters	D_2h, $^1A_{1g}$[b] Min	C_2v, $^3A_2$ Min	D_2h, $^3A_{1u}$ TS(287.4)[a]	D_2h, $^3B_{2u}$ Min	D_2h, $^1A_{1g}$ TS(362.9)[a]	C_2v, $^3A_2$ Min	D_2h, $^3B_{2u}$ Min $\langle S^2\rangle = 2.2$
SI1−SI2	2.327	2.583	2.583	2.593	2.327	2.327	2.590
SI1−C3	1.788	1.805	1.824	1.839	1.799	1.788	1.831
C3−C4	2.716	2.576	2.576	2.608	2.739	2.716	2.589
C3−H5	1.065	1.071	1.071	1.072	1.018	1.065	1.083
SI1−C3−SI2	81.1	90.2	90.2	89.7	80.7	81.1	90.0
C3−SI1−C4	98.9	91.1	89.8	90.3	99.3	98.9	90.0

[a] Bond lengths are given in angstroms and angles in degrees; numbering system corresponds to Figure 3. [b] Min indicates a local minimum on the potential energy surface; TS (imaginary frequency in parentheses) indicates a transition state.

Table 3. Geometric Parameters for $C_4H_4Si_4$ at Various Levels of Theory[a,b]

	SCF			MP2		
	RHF		UHF	RMP2		UMP2
parameters	C_2v, $^1A_1$ TS(81.8)	C_2v, $^3A_1$ Min	C_2v, $^3A_1$ Min	C_2v, $^1A_1$ Min	C_2v, $^3A_1$ Min	C_2v, $^3A_1$ Min
SI1−SI2	2.671	3.514	2.781	2.706	3.502	3.515
SI3−SI4	2.705	2.756	2.724	2.693	2.689	2.703
SI1−C5	1.836	1.975	1.842	1.846	1.976	1.979
SI1−C7	1.920	1.943	1.898	1.901	1.892	1.903
SI3−C7	1.923	1.941	1.930	1.920	1.929	1.935
C5−C6	1.709	1.609	1.647	1.701	1.591	1.781
C7−C8	2.561	2.655	2.570	2.573	2.710	2.707
C6−H10	1.071	1.076	1.075	1.086	1.088	1.088
C7−H11	1.082	1.075	1.083	1.093	1.087	1.087
C5−SI1−C6	55.5	48.1	53.1	54.9	47.5	47.2
SI1−C5−SI2	93.4	125.7	98.1	94.3	124.8	125.3
SI4−C7−SI3	105.4	90.4	89.8	89.1	88.4	88.6
C7−SI3−C8	83.6	86.3	83.5	84.1	89.2	88.7
SI1−C7−SI3	105.5	89.2	129.6	105.5	90.3	89.9
SI1−C5−C6−SI2	−110.6	−153.9	−115.2	−111.4	−151.1	−151.5
C7−SI3−SI4−C8	139.3	−152.1	140.2	140.1	156.7	−155.3

[a] Bond lengths are given in anstroms and angles in degrees. [b] Min indicates a local minimum on the potential energy surface; TS indicates a transition state (imaginary frequency in parentheses).

unrestricted Hartree−Fock (UHF) and restricted open-shell Hartree−Fock (ROHF) methods, for comparison purposes.

Thermochemical predictions for benzene are not as accurate as those for smaller compounds.[10d,16] "Conventional" G2 underestimates the standard heat of formation of benzene by 3.9 kcal mol^{-1}, while G3 is only in error by −0.6 kcal mol^{-1} relative to the experimental value.[10d] In the current study, the G2 energies were used in combination with the experimental atomization energies to calculate the standard heats of formation. This method gives quite good agreement with experiment for most cases, except for aromatic systems, as can be seen from Table 4. Diacetylene, benzene, and phenylacetylene were also calculated via the isodesmic reactions proposed by Raghavachari.[16] For example, the following isodesmic reaction can be written for benzene:

R1: $$C_6H_6 + 6CH_4 \rightarrow 3C_2H_4 + 3C_2H_6$$

(16) Raghavachari, K.; Stefanov, B. B.; Curtiss, L. A. *J. Chem. Phys.* **1997**, *106*, 6764.

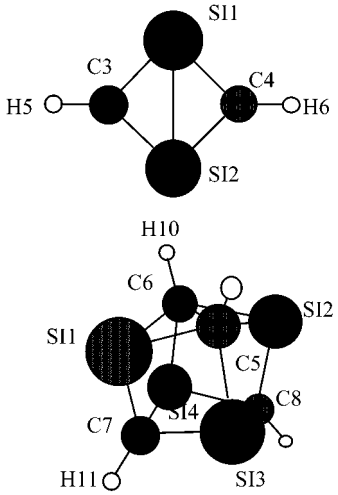

Figure 2. Connectivity of atoms in the Si-doped fragments $C_2H_2Si_2$ and $C_4H_4Si_4$. See Table 1 for geometries.

Table 4. Zero-Point Corrected Energies and Heats of Formation of the Primary Fragments

Molecule	E_0[G2(MP2,SVP)]	ΔH_f^0(298.15)[a]	$\Delta H_f^{0,\,exp,a}$
H	-0.500000[b]	--	52.10316
C	-37.782330[b]	--	171.288
SI	-288.930360[b]	--	108.0±2.0
H_2	-1.166112	-0.9	0.0
CH_4	-40.407968	-18.0	-17.8951
C_2H_2	-77.184449	54.1	54.19010
C_2H_4	-78.412567	12.4	12.53990
C_2H_6	-79.626068	-20.1	-20.04±0.07
C_4H_2	-153.203839	108.4 108.7[c]	110.0
C_6H_6	-231.777710	16.8 18.5[c]	19.82±0.12
	-307.806191	65.2 68.20[c]	73.27±0.64
$C_2Si_2H_2$ (S=0)	-655.258267	133.5	--
$C_2Si_2H_2$ (S=1,UHF)	-655.242046	143.4	--
$C_2Si_2H_2$ (S=1,ROHF)	-655.242555	143.0	--
$C_4Si_4H_4$ (S=0)	--	--	--
$C_4Si_4H_4$ (S=1,UHF)	-1310.613697	204.1	--
$C_4Si_4H_4$ (S=1,ROHF)	-1310.691694	191.9	--

[a] In kcal mol^{-1}. [b] From ref 5c. [c] Computed from appropriate homodesmic reactions.

This method underestimates the value for benzene by only 1.4 kcal mol^{-1} at the G2(MP2,SVP) level of computation.

The G2(MP2, SVP) energies of the fragments F3 and F4 (see Figure 1) of the homodesmic reaction could not be directly computed, due to linear dependencies caused by the diffuse functions at the *E*[MP2/6-311+G(3df,2p)] step. In analogy with benzene, the heats of formation of these fragments were therefore computed indirectly using the following isodesmic schemes at the MP2/6-31G(d) level of theory:

R2: $\mathrm{Ph{-}C{\equiv}C{-}Ph}\ (F3) + 4CH_4 \rightarrow 2\,C_6H_6 + C_2H_2 + 2C_2H_6$

R3: $\mathrm{HC{\equiv}C_a{-}Ph{-}C{\equiv}C{-}CH}(F4) + 6CH_4 \rightarrow C_6H_6 + 3C_2H_2 + 3C_2H_6$

B. $C_{36}H_{16}$. The ground state (^{1}A) of $C_{36}H_{16}$ has a chiral conformation with D_2 symmetry. MNDO-PM3[1] calculations predict a barrier of 7.5 kcal mol^{-1} for enantiomerization through a planar D_{2h} structure. In this work, the planar structure is also predicted to be a transition state, with one very small imaginary frequency of 10.84i cm^{-1}. The energy difference between the D_2 minimum and the D_{2h} transition state is calculated to be 7.4 kcal mol^{-1} at the MP2/6-31G(d) level using RHF geometries, corrected for vibrational zero-point energies by the scaled harmonic Hartree−Fock frequencies. Figure 3 shows a set of selected parameters for these two structures.

Onionlike nanotubes are noncrystalline materials with basic units of graphene layers embedded between clusters of sp^3-hybridized C. This mixed hybridization of C's is one of their basic characteristics.[6] $C_{36}H_{16}$ has a graphene-like isomer (tetrabenzo[*bc*,*ef*,*kl*,*n*,*o*]coronene, Figure 4) which is more stable by 328.0 kcal mol^{-1} (G2(MP2/SVP standard heats of formation) than its annulenic derivative.

In Figure 4, the average geometrical parameters of the "graphitic" isomer $C_{36}H_{16}$ are given, as well as the isodesmic scheme used in the computation of its heat of formation.

C. Si Doping and Structural/Electronic Effects. Given the evasiveness of silicon-containing species with multiple bonds, only four carbon atoms were substituted in the parent molecule, and in such a way that the linear diacetylenic C_4 units have single bonds between Si and Si. Schematically:

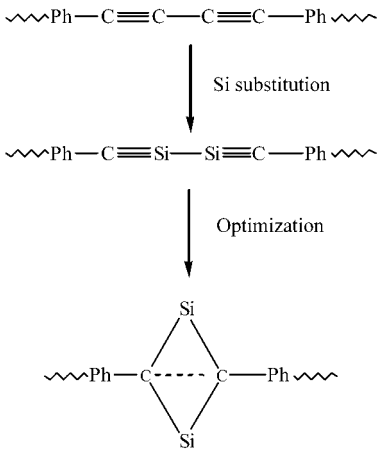

Optimization of the silicon system led to a twisted structure as for the all-C species, except that the originally linear Si−C bonds rearranged to form two C_2Si_2 diamond-shaped rings, due to the instability of the Si−C multiple bonds[17,18]

(17) (a) Schaeffer, H. F. III *Acc. Chem. Res.* **1982**, *15*, 283. (b) Baldridge, K. K.; Boatz, J. A.; Koseki, S.; Gordon, M. S. *Annu. Rev. Phys. Chem.* **1987**, *38*, 211.

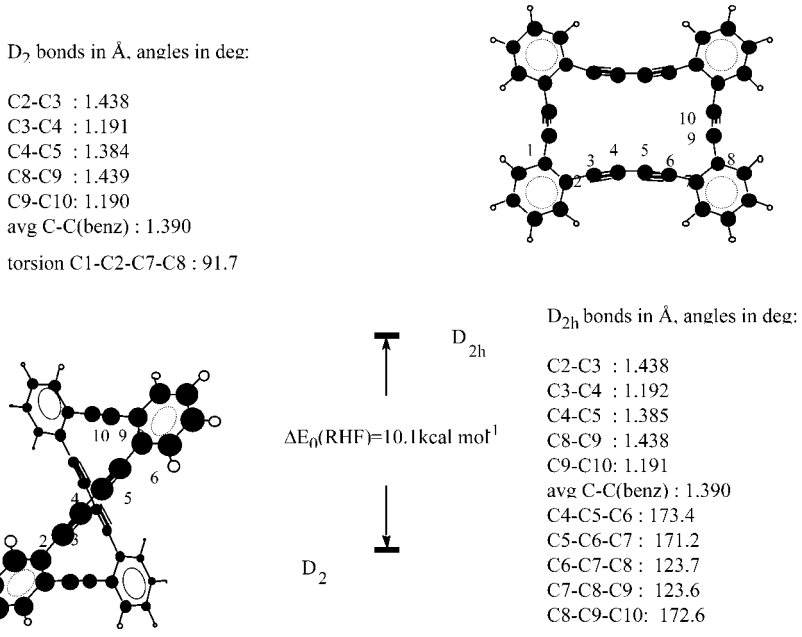

Figure 3. RHF geometrical parameters for the ground and transition states for $C_{36}H_{16}$.

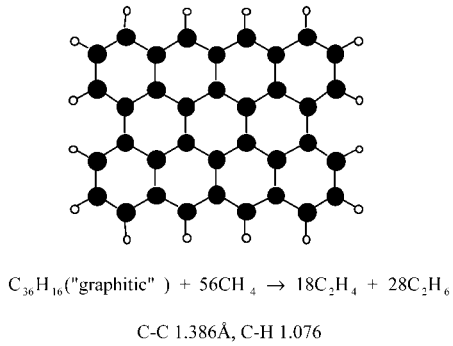

Figure 4. Selected RHF geometric parameters and isodesmic reaction for the graphene isomer.

As Murrel et al. first pointed out,[18a] the isomerization of silaacetylene to :Si═CH_2 is substantially exothermic. Hopkinson and Lien[18b] discovered that the linear HSiCH is not even a minimum on the potential surface. However, Gordon and Pople[18c] and Schaeffer[18d] found that a slightly bent structure of silaacetylene is in fact favored. These findings are in accord with the results for $C_{32}Si_4H_{16}$. Three minimums were located on the Hartree−Fock potential energy surface (PES). All structures are stationary points with positive definite Hessians. The triplet was optimized within the restricted open-shell method. The Cartesian coordinates of the optimized geometries can be obtained upon request.

One local minimum is a D_2 ^{1}A state (Figure 5a). A second local minimum is a C_1 ^{3}A state (Figure 6a). Since the two structures are considerably different, the singlet state was reoptimized starting from the triplet geometry. This led to a C_1 ^{1}A structure that is lower in energy than D_2 ^{1}A (Figure 7a). This minimum is more stable by 50.3 kcal mol^{-1} than the D_2 singlet state and 18.9 kcal mol^{-1} more stable than the triplet at the MP2/6-31G(d)//HF/6-31G(d) level of theory including zero-point corrections. The main difference between the D_2 and C_1 structures is the collapse of the C_2Si_2 ring in the interior of the molecule to form a C_4Si_4 core. Note, however, that while the

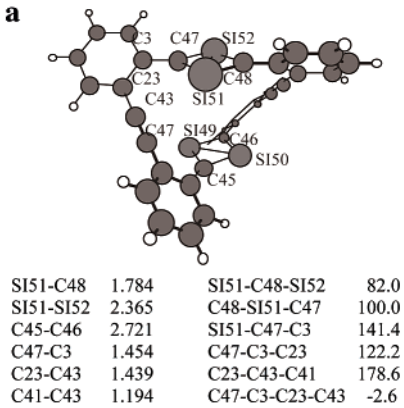

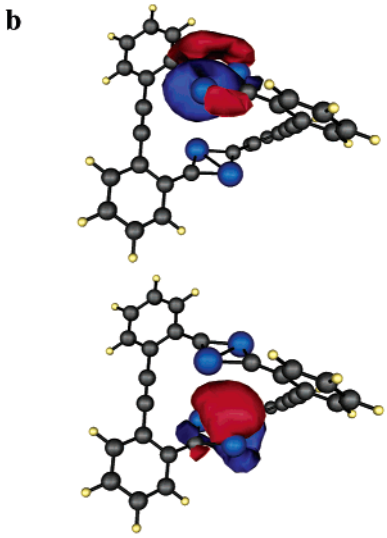

Figure 5. (a) Selected RHF geometric parameters for the D_2 ^{1}A state of $C_{32}Si_4H_{16}$; (b) localized molecular orbitals for the ^{1}A state of $C_{32}Si_4H_{16}$. Bond distances in angstroms; angles in degrees.

(18) (a) Murrel, J. N.; Kroto, H. W.; Guest, M. F. *J. Chem. Soc., Chem. Commun.* **1977**, 619. (b) Hopkinson, A. C.; Lien, M. H. J. *Chem. Soc., Chem. Commun.* **1980**, 107. (c) Gordon, M. S.; Pople, J. A. *J. Am. Chem. Soc.* **1981**, *103*, 2945. (d) Schaeffer, H. F., III. *Acc. Chem. Res.* **1982**, *15*, 283.

a

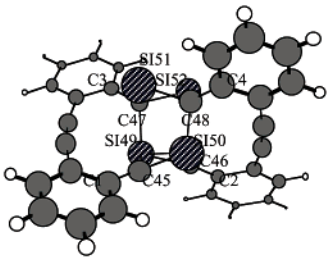

C45-SI50	1.834	C45-C1	1.459	C41-C43-C23	169.3
C45-SI49	1.944	C46-C2	1.451	C42-C44-C24	170.8
C46-SI50	1.833	C47-C3	1.506	C21-C1-C5	117.9
C46-SI49	1.945	C48-C4	1.506	C21-C17-C13	120.7
C47-SI51	1.900	C41-C43	1.194	C17-C13-C9	119.7
C47-SI52	1.920	C42-C44	1.196	C1-C5-C9	121.4
C47-C48	2.631	C21-C1	1.413	C22-C2-C46	120.3
C48-SI50	1.890	C21-C17	1.392	C21-C1-C45	121.9
C48-SI51	1.945	C17-C13	1.380	C4-C24-C44	117.8
C48-SI52	1.982	C1-C5	1.397	C24-C4-C8	117.2
SI47-C47	2.006	C22-C2	1.415		
SI47-SI50	2.498				

b

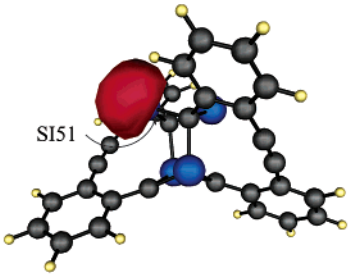

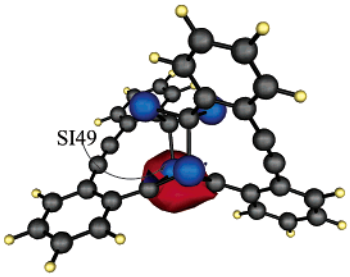

c

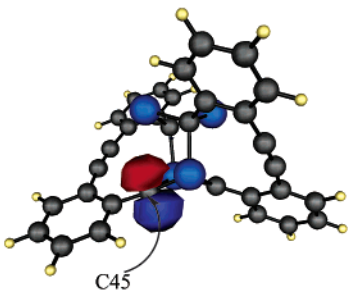

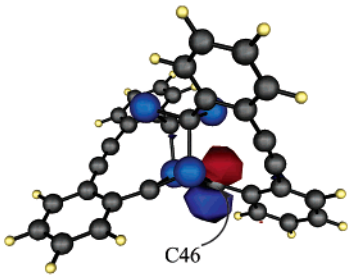

Figure 6. (a) Selected RHF geometric parameters for the C_1 ^3A state of $C_{32}Si_4H_{16}$; (b, c) localized molecular orbitals for the ^3A state of $C_{32}Si_4H_{16}$. Bond distances in angstroms; angles in degrees.

a

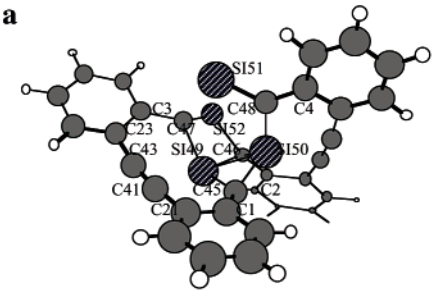

C47-C3	1.487	SI49-C47-SI50	90.0
C47-SI52	1.929	C47-SI52-C46	86.3
C48-CI50	1.815	SI49-C46-SI52	88.9
C48-SI51	1.784	C46-SI49-C47	88.1
SI49-C45	1.776	SI50-C48-SI51	113.3
SI49-C46	1.917	C48-C50-SI49	108.9
SI49-C47	1.859	C50-C46-SI49	74.8
SI49-SI50	2.315	C21-C41-C43	171.3
C21-41	1.431	C46-SI49-C47-SI52	-152.2
		SI50-C46-SI49-C45	-29.7
		C21-C41-C43-C23	-7.9

b

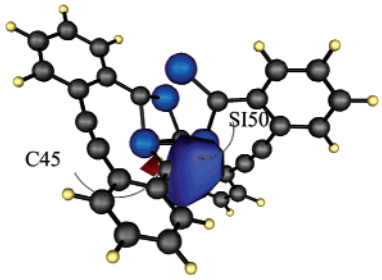

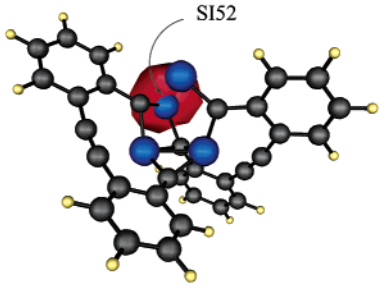

c

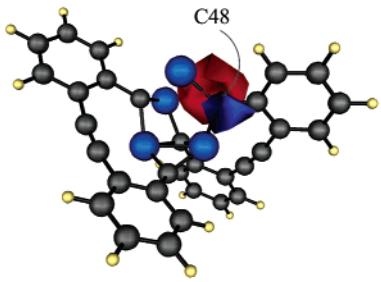

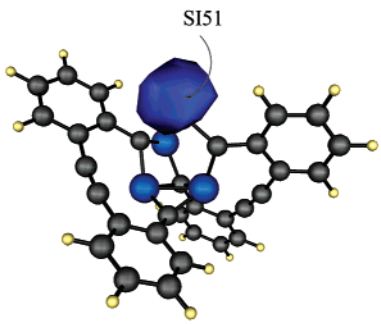

Figure 7. (a) Selected RHF geometric parameters for the other singlet (C_1) state of $C_{32}Si_4H_{16}$; (b, c) localized molecular orbitals. Bond distances in angstroms; angles in degrees.

Table 5. Energies (in Hartrees), Zero-Point Energies, and Standard Heats (Gas) of Formation (in kcal mol^{-1})

Molecule	E_0(MP2)	$\Delta H_f^{0,298.15}$
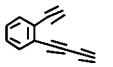	-459.095388	175.7
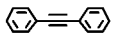	-537.506636	87.9 (Exp 92.0±0.64[a])
$C_{36}H_{16}$ (D_2, S=0)	-1376.415431	385.7
$C_{36}H_{16}$ (D_{2h}, S=0)	-1376.403616[b]	{393.2}[b]
$C_{36}H_{16}$ (graphitic sheet) (D_{2h}, S=0)	-1376.877380	44.2
$C_{32}Si_4H_{16}$ (D_2, S=0)	-2380.475330	413.3
$C_{32}Si_4H_{16}$ (C_1, S=0)	-2380.555493	--
$C_{32}Si_4H_{16}$ (C_1, S=1)[c]	-2380.525448	668.3[d]
$C_{72}H_{36}$ (D_2, S=0)	-2752.890425	[707.6][e]

[a] From ref 20. [b] Only ($3N - 7$) normal modes were included in the correction of the transition state. The computed heat of formation corresponds to H^0_f(0 K). [c] *S* denotes the multiplicity of the state, for $S = 1$, restricted open-shell calculation was performed. [d] Computed from isodesmic reaction, using ROHF energies and experimental heats of formation of the fragments where available. [e] The estimate here is given for comparison, as this number was computed from the dimerization reaction and not any iso- or homodesmic reaction.

central cluster maintains an almost C_{2v} local symmetry in the case of the triplet state, it adopts a highly asymmetric conformation in the singlet with one dangling bond: Si-51 is connected only to C-48 with an almost double bond (bond order 1.428). In the case of the triplet, Si-51 is connected to both C-48 and C-47 (Figure 6a).

The standard heat of formation (Table 5) of the Si-doped species was calculated via the following isodesmic reactions, at the MP2/6-31G(d)//HF/6-31G(d) level of theory

R4 (D_2, singlet): $C_{32}Si_4H_{16} + 8CH_4 \rightarrow$
$2\text{Ph-C}\equiv\text{C}-\text{Ph} + 2C_2Si_2H_2 + 4C_2H_6$

R5 (C_1, triplet): $C_{32}Si_4H_{16} + 8CH_4 \rightarrow$
$2\text{Ph-C}\equiv\text{C}-\text{Ph} + C_4Si_4H_4 + 4C_2H_6$

D. Dimerization of $C_{36}H_{16}$. UV (337 nm N_2 laser) laser desorption time-of-flight (LD-TOF) and IR laser desorption Fourier transform mass spectroscopy (LD-FTMS) experiments[1] on films of $C_{36}H_{16}$ indicate that the initial stages of its explosive transformation are very likely to involve oligomerization to up to 20 units. This idea was tested by exploring the dimerization of the parent system, as this would provide an estimate of the stability of the simplest oligomer (the dimer) and therefore an indication of the feasibility of such a process. The resulting dimer has a total of 1144 basis functions at the RHF/6-31G(d) level of theory, at which first and numerical second derivatives were computed. To conserve computer time, the symmetry was constrained to D_2, as in the monomer, resulting in 26 symmetry unique atoms and a total of 104 atoms (72 heavy).

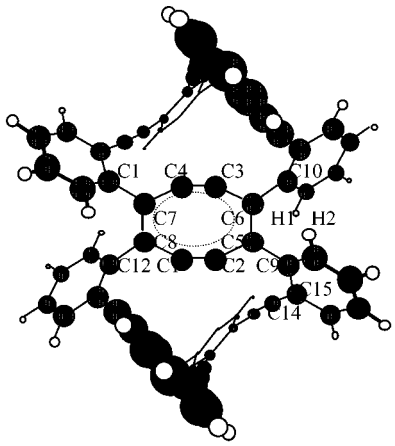

C1-C2	1.192	C1-C8-C12	121.7
C1-C8	1.459	C1-C2-C5	155.3
C6-C10	1.494	C2-C5-C6	114.6
C7-C8	1.353	C5-C6-C8	123.6
C9-C10	3.022	C1-C2-C5-C9	57.5
H1-H2	4.063	C5-C9-C13-C14	-0.42
		C9-C5-C6-C10	15.1

Figure 8. Selected geometric parameters of $C_{72}H_{32}$ dimer. Bond distances in angstroms; angles in degrees.

The diacetylenic side units were chosen as the dimerization sites, as can be seen in Figure 8. The choice was based on suggestions (ref 16 and refs therein) that polyacetylenes easily undergo side polymerization compatible with mild heating in vacuo that triggers the explosive transformation. The following schematic depicts the reaction across the diacetylenic sides of the two monomers, where the triple bonds open up in order to form an eight-membered ring between two allenic-type units:

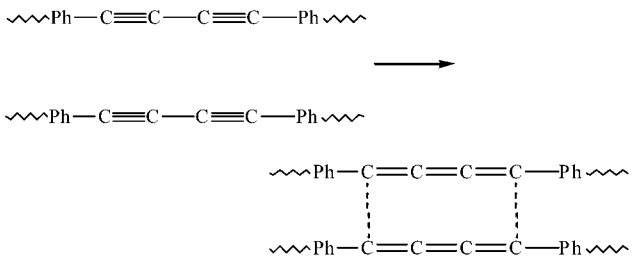

Because of the strain in the resulting eight-membered ring, the final optimized geometry (D_2) acquires the following structure along the periphery of the eight-membered ring:

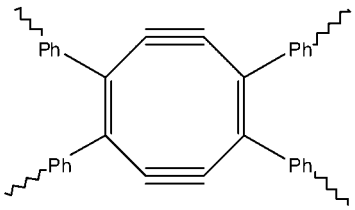

At the MP2/RHF//(6-31G(d) level of theory, including scaled RHF ZPE corrections, the dimer is lower in energy than two monomer units ($C_{36}H_{16}$) by 37.4 kcal mol^{-1}.

Table 6. Singlet−Triplet Splittings, and First Koopmans Ionization Potentials

molecule	$\check{E}$(singlet–triplet)[a]	1st Koopmans[b]
$C_{36}H_{16}$ (D_2)		7.8
$C_{36}H_{16}$ (D_2h)$_{(graph)}$		5.1
$C_{32}Si_4H_{16}$ ($S = 0$, D_2)	+31.5	6.7
$C_{32}Si_4H_{16}$ ($S = 0$, C_1)	−18.9	6.6
$C_{32}Si_4H_{16}$ ($S = 1$, C_1)		3.3

[a] Energy differences taken as (singlet−triplet) in kcal mol^{-1}, at MP2/HF//6-31G(d), corrected for vibrational zero-point energy. [b] In eV.

Discussion

A. Structures and Relative Energies. Table 1 lists the MP2 structures for the references species. Table 2 lists the optimized geometries of the singlet and triplet states of $C_2Si_2H_2$ at the RHF, ROHF, and UHF levels. Due to the considerable spin contamination (∼10%) and the variation in the equilibrium structures with the point group and level of correlation, and given the importance of the G2 method for thermochemical predictions, a restricted-G2 (R-G2) approach is used here, in which UHF/UMP2 are substituted by ROHF/ROMP2 and QCISD(T) is substituted by CCSD(T).

The system $C_2Si_2H_2$ is a particularly interesting prototype for CVD processes. It is a highly unsaturated system with a number of energetically similar, but structurally diverse isomers. Understanding the bonding in this prototype could be quite important for tailoring Si-doped nanostructures. The slightly negative LUMO eigenvalue and the asymmetric character of the localized orbitals, even though the system itself posseses C_{2v} symmetry, are indicative of multireference character. A more detailed study of this system will be forthcoming.[22] For now, we note the considerable difference between restricted and unrestricted geometries at both the Hartree−Fock and MP2 levels of theory (Table 2). In particular, the D_{2h} structure is predicted to be a minimum by UMP2 but a transition state by RMP2.

Table 3 lists the equilibrium geometrical parameters of the singlet and triplet states of the dimer $(C_2Si_2H_2)_2$ at the RHF/MP2, UHF/UMP2 and ROHF/ROMP2 levels. In this system, the differences in the geometric parameters between the HF restricted and unrestricted methods for the triplet are more pronounced than in the case of the monomer. In particular, the predicted symmetry depends on whether UHF or ROHF is used. For example, the ROHF triplet monomer (Table 2) has a C_{2v} minimum and a D_{2h} transition state, whereas the D_{2h} structure is a UHF minimum.

Figure 3 summarizes the equilibrium geometric parameters and barrier to isomerization of the all-carbon system. The planar structure is a transition state with one 10.84i cm^{-1} imaginary frequency and a barrier of 7.4 kcal mol^{-1} at the MP2 level, including the ZPE corrections. The graphene-like isomer (Figure 4) is more stable than the D_2 isomer by 328 kcal mol^{-1} at the MP2 + ZPE level.

Figures 5a, 6a, and 7a list the equilibrium geometric parameters for the three Si-substituted isomers of $C_{32}Si_4H_{16}$. Table 6 lists the triplet−singlet splittings for these isomers. Although the two singlet states are on either side of the triplet energetically, they have essentially the same ionization potential (IP). The presence of Si in the triplet reduces the IP by as much as half the value of the singlet states and is considerably smaller than that of the delocalized graphene structure. The singlet−singlet splitting is 50.4 kcal mol^{-1}.

B. Standard Heats of Formation. The agreement between the calculated heats of formation of the primary fragments and the available experimental data (Table 4) is quite good. For aromatic systems, as observed by others, the direct evaluation of heats of formation from the G2 energy is less accurate than indirect computation via isodesmic reactions where G2 energies are used on both sides of the reaction. The presence of one benzene ring induces a discrepancy of ∼11% from direct evaluation. Use of the appropriate isodesmic scheme reduces this difference to ∼7%.

For the Si-containing species, there are no available experimental data. Si substitution in the fragment species (Table 4) appears to increase the heat of formation of the system by ∼15.0 kcal mol^{-1} per Si atom.

The calculated heat of formation (Table 5) for the $C_{36}H_{16}$ annulenic system (which has been synthesized[1]) is 372.4 kcal mol^{-1}. For the planar transition state, the value in brackets corresponds to the gas standard heat of formation at 0 K. The "graphitic" isomer has a computed heat of formation of 44.0 kcal mol^{-1}. As in the smaller Si-substituted systems, the various $C_{32}Si_4H_{16}$ isomers show the corresponding increase in the heat of formation (Table 5). Notice that two different isodesmic reactions have been used (R4 and R5) depending on the local conformation of the C_2Si_2 units. The heat of formation of the higher singlet (D_2) climbs to 413.3 and 668.3 kcal mol^{-1} for the triplet (C_1) compared to 372.4 kcal mol^{-1}. For the lower singlet, no thermochemical prediction was possible since the central cluster of C_4Si_4 has dangling bonds and would not be well represented by any isodesmic or homodesmic scheme. For the triplet, the computation was done using only ROHF energies. Note that the formation of the $>C_4Si_4<$ "core" in this system increases the heat of formation even more. Also, for the $C_4Si_4H_4$ fragments, the computed heats of formation are more sensitive to the differences between UHF- or ROHF-based methods. This may be due to the larger number of heavy atoms or the structure (cage) of these systems. Unfortunately, there are not enough data in the literature to give some conclusive evidence for either.

C. Localized Orbitals and Localized Charge Distribution (LCD) Energy Decomposition. Figures 5b, 6b and 6c, and 7b and 7c show selected localized molecular orbitals of D_2 singlet, C_1 triplet, and C_1 singlet $C_{32}Si_4H_{16}$. Figure 5b shows the localized orbitals of the four-membered Si_2C_2 units of the D_2 singlet structure. The orbitals are delocalized over the rings very much as in the individual $C_2Si_2H_2$ units, and therefore, the use of isodesmic reaction R4 is justified. Although the isodesmic scheme R4 is used for the C_1 triplet, the localized orbital picture is quite different. In the annulenic system, Si-49. and Si-51 are the least obstructed sites and carry the lone pairs (Figure 6c), while C-45 and C-46 (Figure 6b) carry the unpaired electrons in basically π-type orbitals. In the isolated $C_4Si_4H_4$, there is no steric hindrance and upon localization the unpaired electrons remain mainly on the Si's rather than the C's. The latter, being more electronegative, carry the lone pairs. Indeed, application

(19) For example: Chance, R. R.; Patel, G. N.; Turi, E. A.; Khanna, Y. P. *J. Am. Chem. Soc.* **1978**, *100*, 1307.
(20) Chase, M. W., Jr. *NIST-JANAF Thermochemical Tables*, 4th ed. *J. Phys. Chem. Ref. Data* Monograph 9. **1998**, 1−1951.
(21) England, W.; Gordon, M. S. *J. Am. Chem. Soc.* **1971**, *93*, 4649.
(22) Glezakou, V.-A.; Gordon. M. S., paper in preparation.

of the LCD model of energy decomposition[21] following the localization, confirms that atoms C-45 and C-46 carry one electron each. In the case of $C_4Si_4H_4$ (Figure 2), atoms Si-1, Si-2, C-7, and C-8 share one electron (0.25 e^- each), and Si-3 and Si-4 share the remaining unpaired electron (0.5 e^- each). Apparently, this is a structural effect on the electronic distribution of the molecule. Singlet coupling these unpaired electrons results in the structure shown in Figure 8a, the most stable of all $C_{32}Si_4H_{16}$ isomers.

Conclusion

The standard heats of formation of various annulenic systems are calculated at the G2(MP2,SVP) level of theory. The parent molecule of the series, $C_{36}H_{16}$, is a rather stable system, which undergoes a dramatic transformation to nanostructures upon mild heating. According to the calculations, its energetic content is10.3 kcal mol^{-1}/heavy atom. Partial selective substitution by Si atoms lowers this number to 7.5 kcal mol^{-1}/heavy atom. Therefore, this type of system may represent a possible precursor for Si-doped nanostructures.

The triplet state of the Si-doped annulene has a predicted Koopmans theorem ionization potential that is 50% smaller than those of the singlet states. An interesting potential application of annulenic-type molecules is their use as molecular switches,[23] in the computer chip industry. Fairly small singlet−triplet splittings as in the case of $C_{32}Si_4H_{16}$, or the very low barrier to isomerization between two chiral structures as in the case of $C_{36}H_{16}$, suggests that these systems may also be good candidates for such uses.

Acknowledgment. The authors acknowledge Dr. M. W. Schmidt for many helpful discussions and the Scalable Computing Laboratory of Ames Laboratory for making computing resources available. Part of the computations, without which this project could have been completed, were performed at the Aeronautical Systems Center, Maui High Performance Computing Center and Engineering Research and Development Center under a DoD Challenge Project Grant. This project was also supported by AFOSR Grant F49620-99-1-0063.

Supporting Information Available: Table of the energies used for the computation of the G2(MP2,SVP) energies (PDF). This material is available free of charge via the Internet at http://pubs.acs.org.

JA012301U

(23) (a) Irie, M. *Chem. Rev.* **2000**, *100*, 1685. (b) Diederich, F. *Ang. Chem. (Eng.)* **1999**, *38*, 674.